Time Evolution of the Bootstrap Current Profile in LHD Plasmas

Yuji Nakamura 1), K. Y. Watanabe 2), K. Kawaoto 1), K. Ida 2), Y. Narushima 2), M. Yoshinuma 2), S. Sakakibara 2), I. Yamada 2), T. Tokuzawa 2), M. Goto 2), K. Tanaka 2), N. Nakajima 2), K. Kawahata 2), and LHD experimental group

1) Graduate School of Energy Science, Kyoto University, Uji, Kyoto 611-0011, Japan
2) National Institute for Fusion Science, Toki, Gifu 509-5292, Japan

e-mail contact of main author: nakamura@energy.kyoto-u.ac.jp

Abstract. The direction of the bootstrap current is inverted in the outward shifted plasmas of the Large Helical Device (LHD). In order to verify the reliability of the theoretical models of the bootstrap current in helical plasmas, the rotational transform profiles are observed by the Motional Stark Effect measurement in the bootstrap current carrying plasmas of the LHD, and they are compared with the numerical simulations of the toroidal current profile including the bootstrap current. Since the toroidal current profile is not in the steady state in these plasmas, taking care of the inversely induced component of the toroidal current and finite duration of the resistive diffusion of the toroidal current are important in the numerical simulations. Reasonable agreement can be obtained between the rotational transform profiles measured in the experiments and those calculated in the numerical simulations

1. Introduction

Since the rotational transform profile, which has important roles on the magnetohydro-dynamics (MHD) stability and transport, is sensitive to the net plasma current, it is indispensable to estimate the toroidal current profile quantitatively. In the LHD, Ohmic current is not driven actively by the external circuit, and observed total toroidal current is mainly driven by the non-inductive current, such as the bootstrap current and Ohkawa current. Since the total toroidal current does not reach the steady state in most of the LHD experiments, the current ramp-up due to the non-inductive current induces the toroidal electric field inversely in accordance with Faraday's law. In addition to that, high electric conductivities of plasmas cause slow radial diffusion of the toroidal currents. In order to estimate the toroidal current profile quantitatively, therefore, not only a theoretical model for the non-inductive current but also that for the current profile evolution is required even in helical plasmas, in which the current profile evolutions have not been studied extensively. Otherwise, theoretical models of the non-inductive current, such as the bootstrap current, in helical plasmas cannot be verified properly by the experiments.

It is predicted theoretically for LHD plasmas that the configuration dependence of the bootstrap current is strong in the outward shifted plasmas and it affects the MHD equilibrium limit [1]. In the previous studies, total amount of the bootstrap current was estimated experimentally in the LHD plasmas and compared with that obtained from the theoretical calculation [2]. But there had previously been no experimental estimation of the radial profile of the bootstrap current. The Motional Stark Effect (MSE) measurement is now equipped in the LHD [3], and the rotational transform profile can be measured. Moreover, a numerical simulation code, TASK/EI+BSC [4, 5], is available to calculate the time evolution of the bootstrap current profile consistently with the three-dimensional (3D) MHD equilibrium. The TASK/EI+BSC code solves a time evolution equation of the rotational transform profile, which is equivalent to the toroidal current profile, by the iterative calculation with the 3D MHD equilibrium and the bootstrap current calculations. In this paper, we compare the

rotational transform profile obtained by the MSE measurement and that calculated by the numerical simulation of the toroidal current including the bootstrap current component and the inductive current component.

2. Numerical Simulation of the Toroidal Current Evolution

In the BSC code [6], the bootstrap current is estimated based on the momentum method for asymmetric devices proposed by K.C. Shaing et al. [7, 8], where the linearized drift kinetic equation is solved analytically, and connection formula from 1/ν to Pfirsch-Schülter collisional regime is applied.

A conservation equation of the rotational transform ι is derived from the contravariant component of Faraday's law:

$$\frac{\partial \iota}{\partial t} = \frac{1}{\phi'}\left[\left.\frac{\partial \phi}{\partial t}\right|_s \frac{\partial \iota}{\partial s} + \frac{\partial}{\partial s}\left(\frac{\mathcal{V}'}{\phi'}\eta_{\parallel}\left(\left\langle \mathbf{j}\cdot\mathbf{B}\right\rangle - \left\langle \mathbf{j}_{NI}\cdot\mathbf{B}\right\rangle\right)\right)\right],$$

where $\phi = \Phi_T / 2\pi$, Φ_T is the toroidal magnetic flux, $s \equiv \Phi_T / \Phi_T^{edge}$ is the toroidal flux normalized by its value at the plasma boundary, $\mathcal{V} = V/(2\pi)^2$, V is volume inside the flux surface. Primes denotes derivative with respect to s, $\eta_{\parallel}$ is the neoclassical parallel resistivity, $\langle \mathbf{j}\cdot\mathbf{B}\rangle$ and $\langle \mathbf{j}_{NI}\cdot\mathbf{B}\rangle$ correspond to the flux averaged parallel current density and non-inductive current density, respectively. When we use the relation between $\langle \mathbf{j}\cdot\mathbf{B}\rangle$ and ι, we can obtain,

$$\frac{\partial \iota}{\partial t} = \left(\frac{\phi_a}{s}\frac{\partial \phi_a}{\partial t}\right)\frac{\partial \iota}{\partial s} + \frac{1}{{\phi_a}^2}\left[\frac{\partial}{\partial s}\left\{\eta_{\parallel}\mathcal{V}'\frac{\left\langle B^2\right\rangle}{{\mu_0}^2}\frac{\partial}{\partial s}\left(S_{11}\iota + S_{12}\right)\right\} + \frac{\partial}{\partial s}\left\{\eta_{\parallel}\mathcal{V}'p'\left(S_{11}\iota + S_{12}\right) - \eta_{\parallel}\mathcal{V}'\left\langle \mathbf{j}_{NI}\cdot\mathbf{B}\right\rangle\right\}\right].$$

where $\phi_a = \Phi_T^{edge}/2\pi$, $\langle B^2\rangle$ is flux surface average of the square of magnetic field strength, p is pressure, S_{11} and S_{12} are the susceptance matrix defined in Ref.[9]. This equation is solved in the TASK/EI code with the MHD equilibrium quantities obtained by the VMEC code [10] and non-inductive current (the bootstrap current in the present case) calculated by the BSC code.

The equilibrium and bootstrap current data are supplied to the TASK/EI and the rotational transform is evolved during some time interval, which is typically 100ms for LHD plasmas. In the equation of the rotational transform evolution, we assumed that MHD equilibrium quantities such as susceptance matrix are consistent with evolved ι (in this sense, the equation is intrinsically non-linear), but we also assumed that change of ι and the resultant change of MHD quantities are negligibly small during the time interval. Then, the updated rotational transform profile along with the experimentally obtained density and temperature profiles are used as input of the equilibrium code, and bootstrap current is re-estimated by the BSC again. These procedures are iterated during the simulation.

3. Dependence of the Bootstrap Current Profile on the Plasma Position

In order to verify the capability of the bootstrap current calculation code, BSC code, the total amount of the toroidal current calculated by the BSC code is compared with that estimated experimentally. We estimate the non-inductive current by taking into account of the mutual coupling due to the structure surrounding the plasma, such as coils, vacuum vessel and so on. Figure 1 shows the dependence of the non-inductive current obtained experimentally on the magnetic configurations with different magnetic axis. The volume averaged beta values are

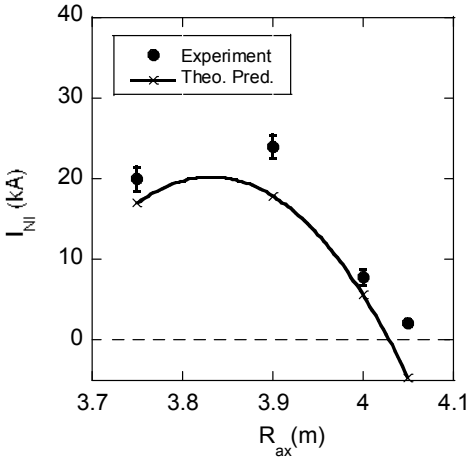

Fig.1 The magnetic axis position dependence of the non-inductive current obtained experimentally and the comparison between experimental results and the theoretical prediction.

almost same, $<\beta_{dia}>$=0.33~0.41%. The data are obtained under the same condition of NB injection; co NB has the port through power of 2MW with beam energy of 150keV, and two counter NBs have 0.6MW with 120keV and 1MW with 150keV, respectively. Circles denote the experimental data and a line denotes the theoretical prediction of the bootstrap current by the BSC code. We find that the bootstrap current is the most probable candidate as a driving mechanism of the non-inductive current in LHD experiments under the balanced NB injection.

The rotational transform profile is measured by the MSE in LHD plasmas of which vacuum magnetic axis position are R_{axis}=3.9m. Time evolution of this discharge is shown in Fig.2. In this NB balanced injection discharge, $<\beta_{dia}>$~0.5% and the total toroidal current reaches around 10kA. Figure 3 shows time evolution of the electron density and temperature profiles of this discharge obtained from the experiment. In Fig.3, the radial variable $\rho \equiv s^{1/2}$ corresponds to the representative normalized minor radius. The electron density has a rather flat or hollow profile. The electron temperature has a bell-shaped profile and its profile is almost constant in time. Figure 3 also shows a pressure profile when we

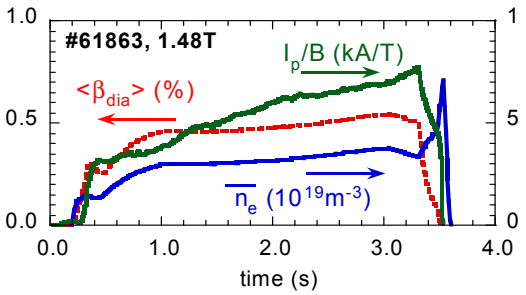

Fig.2 Time evolution of experimentally observed electron densities, volume averaged beta, and the total plasma current for R_{axis}=3.9m case.

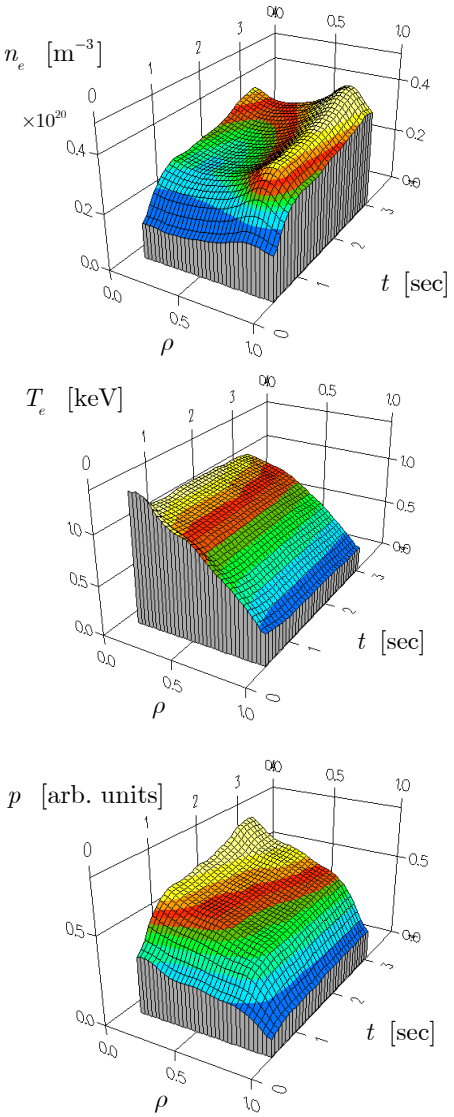

Fig.3 Time evolutions of electron density profile, electron temperature profile, and pressure profile measured in the experiment for R_{axis}=3.9m case shown in Fig.2.

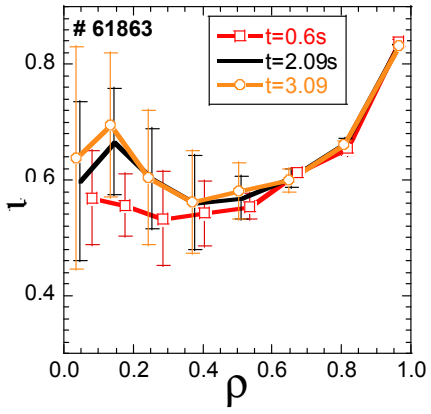

Fig.4 Time evolution of the rotational transform profile obtained by the MSE measurement for R_{axis}=3.9m case.

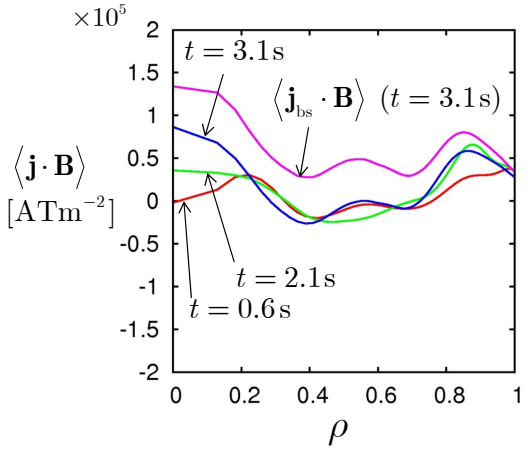

Fig.5 Time evolution of the flux averaged parallel current profile obtained by the numerical simulation for R_{axis}=3.9m case.

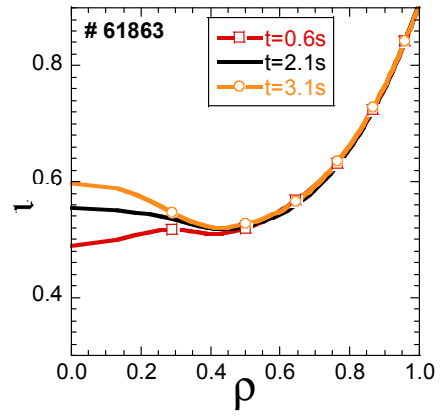

Fig.6 Time evolution of the rotational transform profile obtained by the numerical simulation for R_{axis}=3.9m case.

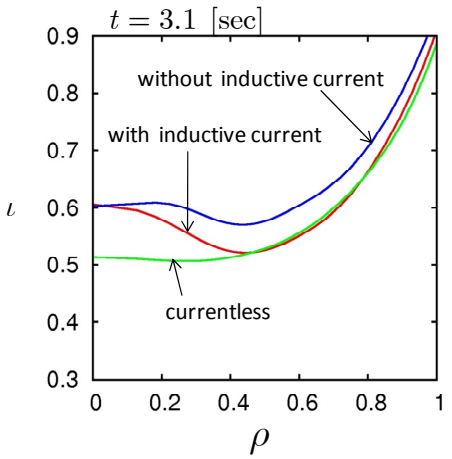

Fig.7 Dependence of the rotational transform profile at t=3.1s on the assumed current profile for R_{axis}=3.9m case.

assume that the ion temperature is equal to the electron temperature. These profiles obtained from the experiment are used in the numerical simulation of the plasma current.

In Fig.4, the rotational transform profiles obtained by the MSE measurement for the R_{axis}=3.9m case corresponding to Figs.3 and 4 are shown. It can be seen from Fig.4 that the central value of the rotational transform is around 0.6, and its minimum is about 0.55 and located around ρ=0.4~0.5. Time evolution of the rotational transform profile is calculated by the TASK/EI+BSC with the VMEC. In this calculation, experimentally estimated time evolution of density and temperature profiles in Fig.3 is used. Measured total current in Fig.2 is also used as a boundary condition of the rotational transform evolution. Figure 4 shows time evolution of the flux averaged parallel current profiles obtained by the numerical simulation. The current density is almost zero around the half radial position and slightly positive near the edge, and it is increased with time near the plasma center. Total current at $t = 3.1\mathrm{s}$ is about 10kA. On the other hand, the bootstrap current calculated by the BSC is positive in the entire region, and total bootstrap current is about 30kA. Corresponding rotational transform profile is shown in Fig.6. This profile does not change in time except for the central region, as same as that in Fig.4 estimated by the MSE measurement. Finally, the

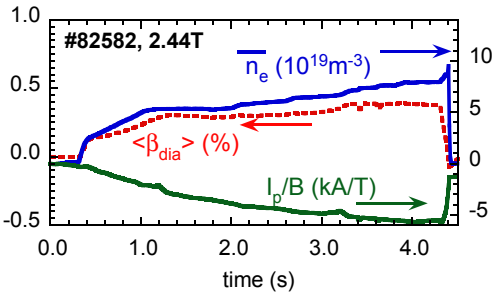

Fig.8 Time evolution of experimentally observed electron densities, volume averaged beta, and the total plasma current for R_{axis}=4.05m case.

rotational transform estimated by the simulation is compared in Fig.7 with those calculated by using two different current profiles. One is that calculated by the VMEC code with the currentless constraint. Another is that obtained from the VMEC equilibrium calculation by taking the bootstrap current into account but neglecting the inverse inductive current. The currentless equilibrium gives the similar rotational transform near the edge, but increase of that near the plasma center cannot be reproduced. If we neglect the inductive current, we cannot explain the small total current and obtain larger rotational transform near the edge. From these results, we can conclude that the numerical result is consistent quantitatively with the measured one for this case.

Since the configuration dependence of the bootstrap current around R_{axis}=4.05m is more sensitive than that around R_{axis}=3.9m, as is shown in Fig.1, dependence of the theoretical model is more pronounced in the R_{axis}=4.05m case. Therefore, this configuration is more suitable to verify the theoretical model for the bootstrap current calculation. Time evolution of this discharge is shown in Fig.8. In this discharge, <β_{dia}>~0.4% and the total toroidal current flows inverse direction compared to the case of R_{axis}=3.9m and reaches around -14kA. Figure 9 shows time evolutions of the electron density

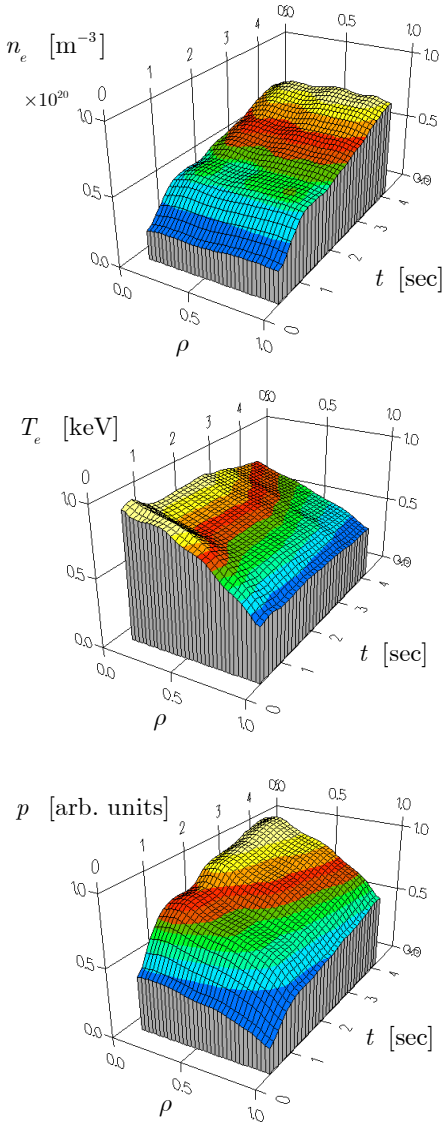

Fig.9 Time evolutions of electron density profile, electron temperature profile, and pressure profile measured in the experiment for R_{axis}=4.05m case shown in Fig.8.

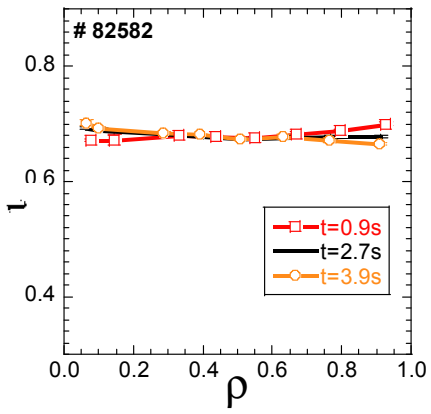

Fig.10 Time evolution of the rotational transform profile obtained by the MSE measurement for R_{axis} = 4.05m case.

profile, temperature profile, and pressure profile of this discharge obtained from the experiment. The electron density profile is quite flat and increases with time. In Fig.10, the rotational transform profiles obtained by the MSE measurement for the R_{axis}=4.05m case corresponding to Figs.8 and 9 are shown. It can be seen from Fig.10 that the rotational transform is almost uniform and its value is around 0.68. It is found from Fig.10 that the rotational transform at the edge decreases in time slightly. This is consistent to the behavior of the total current evolution.

Figure 11 shows time evolution of the flux averaged parallel current profiles obtained by the numerical simulation. The net current is negative except for the central region. The bootstrap current profile shown in Fig.11 has similar profile but total amount of the bootstrap current is about $-5.5\mathrm{kA}$ at $t = 3.9\mathrm{s}$, while the total current observed in the experiment is around $-14\mathrm{kA}$. The result of the time evolution calculation of the rotational transform profile for the configuration with R_{axis}=4.05m, which corresponds to Fig.10, is shown in Fig.12. Both the numerical result and the measured one show flat rotational transform profiles around 0.68. But there is a small difference at the plasma center. As we can see in Fig.13, neglecting the plasma current, i.e. currentless equilibrium, gives larger rotational transform than the MSE measurement on the overall region. Neglecting the inductive current, i.e. considering only the bootstrap current in the MHD equilibrium calculation, gives too large rotational transform at the center. In those sense, the numerical simulation by considering the inductive current shows reasonable agreement with the experimental observation. But more accurate bootstrap current calculation, such as that using the DKES code, is expected to improve the agreement since the theoretical model used in the BSC is not sufficiently accurate when the bootstrap current is nearly zero.

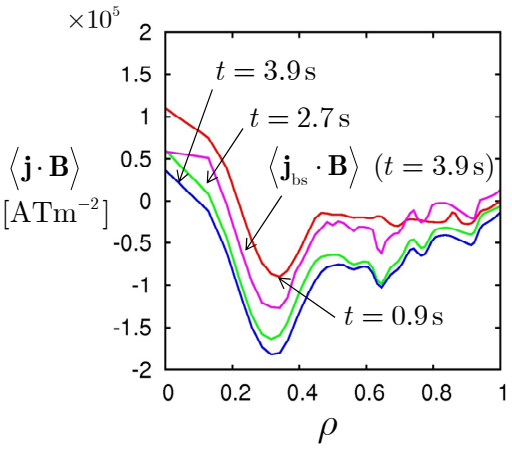

Fig.11 Time evolution of the flux averaged parallel current profile obtained by the numerical simulation for R_{axis}=4.05m case.

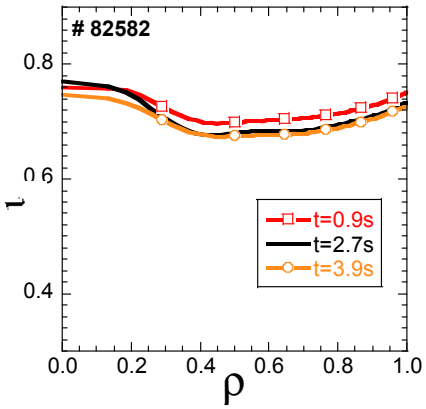

Fig.12 Time evolution of the rotational transform profile obtained by the calculation for R_{axis} = 4.05m case.

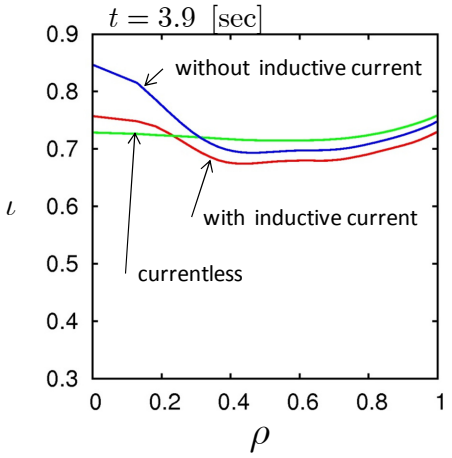

Fig.13 Dependence of the rotational transform profile at t=3.9s on the assumed current profile for R_{axis}=4.05m case.

4. Conclusion

The MSE measurement and numerical simulation of the rotational transform profile are performed in the bootstrap current flowing outward-shifted LHD plasmas. The bootstrap currents estimated by the BSC code increase the rotational transform in LHD plasmas of which vacuum magnetic axis position are R_{axis}=3.9m. Observed net toroidal currents (10kA) are well below the bootstrap currents (30kA), and can be explained by the existence of the inverse inductive currents, which are taken into account in the numerical simulation. If we neglect the net plasma current or inverse inductive current in the equilibrium calculation, the rotational transform profile measured by the MSE cannot be reproduced. Numerical result which is consistent with the experimental observation can be obtained quantitatively.

For the case of R_{axis}=4.05m, negative or subtractive total toroidal currents are observed in the experiment. The direction of the subtractive bootstrap current is opposite to that of the bootstrap currents in tokamaks and corresponds with that in the straight helical plasmas. Theoretical prediction showed that, in L=2 heliotron, the bootstrap current flows opposite direction when the plasma is shifted outward. Therefore, the observation can be explained qualitatively by the bootstrap current calculation by the BSC code. However, the amount of the calculated bootstrap current (−5.5kA) is different from the observed total current (−14kA). This can be also explained by the existence of the inductive current. Since bootstrap current flows in the positive or additive direction at the plasma center but does in the subtractive direction elsewhere than the plasma center in the case of R_{axis}=4.05m, accurate estimations of the bootstrap current are required. In this paper, we found that the numerical simulation preformed by considering bootstrap current estimated by the BSC code and the inductive current shows reasonable agreement with the experimental observation. But more accurate bootstrap current calculation, such as that using the DKES code, is expected to improve the agreement since the theoretical model used in the BSC is not sufficiently accurate when the bootstrap current is nearly zero. That is a future problem we should resolve.

References

[1] K.Y. Watanabe and N. Nakajima, “Effect of bootstrap current on MHD equilibrium beta limit in heliotron plasmas”, Nuclear Fusion **41** (2001) 63.
[2] K.Y. Watanabe et al, J. Plasma Fusion Res. Ser. **5** (2002) 124.
[3] K. Ida, et al., Rev. Sci. Instrum. **76**, 053505 (2005).
[4] Yuji Nakamura et al., Proc. of 21th IAEA Fusion Energy Conf. (Chengdu, China, 2006) IAEA-CN-149/TH/P7-1. 684.
[5] Yuji Nakamura et al., Plasma Fusion Res. **3**, S1058 (2008).
[6] K. Y. WATANABE, et al., Nuclear Fusion **35** (1995) 335.
[7] K. C. Shaing, et al., Phys. Fluids **29** (1986) 521.
[8] K. C. Shaing, et al., Phys. Fluids **B1** (1989) 1663.
[9] P. I. Strand and W. A. Houlberg, Phys. Plasma **8** (2005) 2782.
[10] S. P. Hirshman, W. I. Rij, and P. Merkel, Comput. Phys. Commun. **43** (1986) 143.